Pyrolysis of Polycarbosilanes with Pendant Nickel Clusters: Synthesis and Characterization of Magnetic Ceramics Containing Nickel and Nickel Silicide Nanoparticles

Lars Friebe,[†] Kun Liu,[†] Boris Obermeier,[†] Srebri Petrov,[†] Paul Dube,[‡] and Ian Manners*[,†,§]

Department of Chemistry, University of Toronto, 80 St. George Street, Toronto M5S 3H6, Ontario, Canada, Brockhouse Institute for Materials Research, McMaster University, Hamilton L8S 4M1, Ontario, Canada, and The School of Chemistry, University of Bristol, Bristol BS8 1TS, England

Received October 16, 2006. Revised Manuscript Received February 12, 2007

The synthesis and pyrolysis of a series of soluble, air- and moisture-stable nickel-containing polycarbosilanes (Ni-PCS) is described. The reaction of 1-chloro-1-methyl-silacyclobutane with two different acetylides LiC≡CR (R = phenyl or *tert*-butyl) yielded the silacyclobutane monomers $(CH_2)_3$-SiMe(C≡CR) **2a** (R = Ph) and **2b** (R = *t*-Bu). Pt(0)-catalyzed ring opening polymerization of **2a** and **2b** in the presence of Et_3SiH gave the alkyne-functionalized polycarbosilanes (PCS) $[CH_2-CH_2-CH_2-(Me)Si(C{\equiv}CR)]_n$ **3a** (R = Ph) and **3b** (R = *t*-Bu) with molecular-weight control. The alkyne groups of the PCS polymers were clusterized with cyclopentadienyl nickel groups to yield samples of Ni-PCSs $[CH_2-CH_2-CH_2-(Me)Si(C(NiCp)C(NiCp)R)]_n$ **4a** (R = Ph) and **4b** (R = *tert*-Bu) with molecular weights in the range of $M_n \approx 8000-36\,000$. Pyrolysis of these Ni-PCSs yielded ceramics with embedded Ni or Ni silicide nanoparticles. By adjusting the pyrolysis temperature, it was possible to control the formation of either nickel (400 and 600 °C) or nickel silicide (Ni_3Si and $Ni_{31}Si_{12}$) nanoparticles (900 °C). The substituent group (phenyl or *t*-butyl), the clusterization percentage, and the pyrolysis time all influenced the yield and properties of ceramic materials. The nickel and nickel silicide nanoparticle-containing ceramics were characterized by transmission electron microscopy (TEM), energy-dispersive X-ray analysis (EDX), powder X-ray diffraction (PXRD), and superconducting quantum interference device (SQUID) magnetometry. The blocking temperature (T_B) of the materials was found to strongly depend on the pyrolysis conditions: in the case of the ceramics derived from **4b**, $T_B \approx 10$ K (pyrolysis 600 °C for 1 h), $T_B \geq 325$ K (600 °C, 12 h) and $T_B \approx 135$ K (900 °C, 1 h). Depending on the applied temperature (below or above T_B) the ceramics exhibited either ferromagnetic or superparamagnetic behavior.

Introduction

Metal-containing polymers are of considerable current interest from a material science perspective.[1] The incorporation of transition metals into polymers is relevant for many applications such as catalysis,[2] lithography,[3] uses as redox-active gels,[4] molecular and ion recognition,[5] and the formation of liquid crystalline[6] and supramolecular materials.[7] Beside these applications, transition-metal-containing polymers are important precursors for the generation of metal nanoparticles (NPs), which is achieved via thermal or

* Corresponding author. E-mail: Ian.Manners@bristol.ac.uk.
† University of Toronto.
‡ McMaster University.
§ University of Bristol.

(1) (a) Archer, R. D. *Inorganic and Organometallic Polymers*; John Wiley & Sons Inc.: New York, 2001. (b) Newkome, G. R.; He, E. F.; Moorefield, C. N. *Chem. Rev.* **1999**, *99*, 1689. (c) Astruc, D.; Chardac, F. *Chem. Rev.* **2001**, *101*, 2991. (d) Abd-El-Aziz, A. S., Ed. *Macromol. Symp.* **2003**, *196*, 1. (e) Abd-El-Aziz, A. S., Harvey, P. D., Eds. *Macromol. Symp*. **2004**, *209*, 1. (f) Holliday, B. J.; Swager, T. M. *Chem. Commun.* **2005**, 23. (g) Wolf, M. O. *Adv. Mater.* **2001**, *13*, 545. (h) Manners, I. *Science* **2001**, *294*, 1664. (i) Manners, I. *Synthetic Metal-Containing Polymers*; Wiley-VCH: Weinheim, Germany, 2004.

(2) (a) Ajjou, A. N.; Alper, H. *J. Am. Chem. Soc.* **1998**, *120*, 1466. (b) Peckham, T. J.; Nguyen, P.; Bourke, S. C.; Wang, Q. Y.; Harrison, D. G.; Zoricak, P.; Russell, C.; Liable-Sands, L. M.; Rheingold, A. L.; Lough, A. J.; Manners, I. *Organometallics* **2001**, *20*, 3035. (c) Köllner, C.; Pugin, B.; Togni, A. *J. Am. Chem. Soc.* **1998**, *120*, 10274. (d) Wong, W. Y. J. *Inorg. Organomet. Polym. Mater.* **2005**, *15*, 197. (e) Wong, W. Y.; Ho, C. L. *Coord. Chem. Rev.* **2006**, *250*, 2627. (f) Lastella, S.; Jung, Y. J.; Yang, H.; Vajtai, R.; Ajayan, P. M.; Ryu, C. Y.; Rider, D. A.; Manners, I. *J. Mater. Chem.* **2004**, *14*, 1791.

(3) (a) Clendenning, S. B.; Aouba, S.; Rayat, M. S.; Grozea, D.; Sorge, J. B.; Brodersen, P. M.; Sodhi, R. N. S.; Lu, Z.-H.; Yip, C. M.; Freeman, M. R.; Ruda, H. E.; Manners, I. *Adv. Mater.* **2004**, *16*, 215. (b) Lammertink, R. G. H.; Hempenius, M. A.; Chan, V. Z. H.; Thomas, E. L.; Vancso, G. J. *Chem. Mater.* **2001**, *13*, 429.

(4) (a) Yoshida, R.; Takahashi, T.; Yamaguchi, T.; Ichijo, H. *Adv. Mater.* **1997**, *9*, 175. (b) Arsenault, A. C.; Míguez, H.; Kitaev, V.; Ozin, G. A.; Manners, I. *Adv. Mater.* **2003**, *15*, 503.

(5) (a) Caruana, D. J.; Heller, A. *J. Am. Chem. Soc.* **1999**, *121*, 769. (b) Wang, Z.; McWilliams, A. R.; Evans, C. E. B.; Lu, X.; Chung, S.; Winnik, M. A.; Manners, I. *Adv. Funct. Mater.* **2002**, *12*, 415. (c) Albrecht, M.; van Koten, G. *Adv. Mater.* **1999**, *11*, 171. (d) Wang, B.; Wasielewski, M. R. *J. Am. Chem. Soc.* **1997**, *119*, 12.

(6) (a) Steffen, W.; Köhler, B.; Altmann, M.; Scherf, U.; Stitzer, K.; zur Loye, H.-C.; Bunz, U. H. F. *Chem.—Eur. J.* **2001**, *7*, 117. (b) Oriol, L.; Serrano, J. L. *Adv. Mater.* **1995**, *7*, 348. (c) Hagihara, N.; Sonogashira, K.; Takahashi, S. *Adv. Polym. Sci.* **1981**, *41*, 149. (d) Liu, X. H.; Bruce, D. W.; Manners, I. *Chem. Commun.* **1997**, 289.

(7) (a) Park, C.; McAlvin, J. E.; Fraser, C. L.; Thomas, E. L. *Chem. Mater.* **2002**, *14*, 1225. (b) Wang, X.-S.; Arsenault, A.; Ozin, G. A.; Winnik, M. A.; Manners, I. *J. Am. Chem. Soc.* **2003**, *125*, 12686. (c) Bender, J. L.; Corbin, P. S.; Fraser, C. L.; Metcalf, D. H.; Richardson, F. S.; Thomas, E. L.; Urbas, A. M. *J. Am. Chem. Soc.* **2002**, *124*, 8526. (d) Beck, J. B.; Rowan, S. J. *J. Am. Chem. Soc.* **2003**, *125*, 13922. (e) Eitouni, H. B.; Balsara, N. P. *J. Am. Chem. Soc.* **2004**, *126*, 7446. (f) Lohmeijer, B. G. G.; Schubert, U. S. *Angew. Chem., Int. Ed.* **2002**, *41*, 3825. (g) Chen, B. Z.; Sleiman, H. F. *Macromolecules* **2004**, *37*, 5866. (h) Manners, I. *J. Polym. Sci., Part A: Polym. Chem.* **2002**, *40*, 179.

10.1021/cm062470j CCC: $37.00
Published on Web 04/17/2007

Scheme 1. Polyferrocenylsilanes (PFS) and Cobalt-Clustered Polyferrocenylsilanes (Co-PFS)

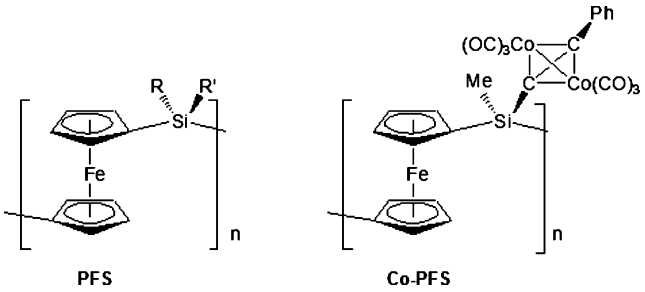

radiation treatment.[8−14] The pyrolysis path usually yields NPs that are contained in a ceramic matrix. The incorporation of transition metals into ceramics is very attractive, as it leads to materials with interesting catalytic, magnetic, electrical, and optical properties.[12,13,15−19] Interesting magnetic properties of NPs are especially relevant with the ferromagnetic transition elements Fe, Co, and Ni.

Our recent studies on the pyrolysis of metal-containing polymers focused on Fe- and Fe/Co-containing polymers such as polyferrocenylsilanes (PFS, Scheme 1),[20] cross-linked PFS,[21] cobalt-clustered polyferrocenylsilanes (Co-PFS, Scheme 1) in bulk,[22] and in the case of Co-PFS, thin films.[23] The pyrolysis of various PFSs at 600−1000 °C affords silicon carbides that contain α-Fe NPs.[20] Related to these investigations, the pyrolysis of hyperbranched PFS gives ceramics containing α-Fe_2O_3 nanocrystals in 50−60% yield as described by Tang et al.[24] Pyrolysis of cross-linked PFS yields shaped macroscopic magnetic ceramics consisting of α-Fe NPs embedded in a SiC/C/Si_3N_4 matrix in greater than 90% yield up to a pyrolysis temperature of 1000 °C.[8,21] The pyrolysis of bulk Co-PFS under N_2 at 600 and 900 °C for 12 h results in magnetic ceramics with relatively high ceramic yields of 72 and 59%, respectively, the analysis of which revealed that CoFe alloy NPs are embedded in an amorphous SiC/C ceramic matrix.[22] Pyrolysis of thin films of Co-PFS leads to the formation of CoFe alloy NPs in ceramic thin films.[23] In addition, as these metallopolymers can be readily patterned using techniques such as electron-beam lithography,[3a] imprinting lithography,[21] UV photolithography[25] and soft lithography,[26] they offer the prospect of accessing patterned arrays of metal and metal alloy NPs for device and catalytic applications.[27] Furthermore, Keller et al. converted linear ferrocenylene-siloxyldiacetylene polymers to Fe-containing ceramics with high thermal and oxidative stabilities.[9]

The generation of Co NPs can be achieved by the pyrolysis of Co-containing polymers. For example, Bunz and coworkers pyrolyzed a dicobalthexacarbonyl-complexed poly(p-phenyleneethynylene) and yielded micrometer-sized carbon−cobalt spheres.[11] Grubbs et al. fabricated carbon nanotubes and Co-based NPs simultaneously by pyrolyzing well-defined diblock copolymers containing Co cluster substituents.[10] Furthermore, other metal NPs, such as Au and Ru NPs, can also be prepared from metallized polymer precursors via electron beam treatment.[28]

In addition to ceramics containing Co, Fe, and CoFe NPs, analogous materials containing Ni NPs are of interest with respect to potential applications in catalysis and as a result of their magnetic properties. Furthermore, from comparisons of Ni, Co, and Fe/Mo as the catalyst material, it has been found that Ni allows the synthesis of single-walled carbon nanotubes in the lowest temperature range.[29] In addition, nickel nanocrystals have been used recently for the growth of germanium nanowires by Korgel et al.[30] Ni NPs are also of interest as nanomagnets for spintronic devices. Studies on the fabrication of Ni NPs through pyrolysis are mainly

(8) (a) MacLachlan, M. J.; Ginzburg, M.; Coombs, N.; Coyle, T. W.; Raju, N. P.; Greedan, J. E.; Ozin, G. A.; Manners, I. *Science* **2000**, *287*, 1460. (b) Temple, K.; Kulbaba, K.; Power-Billard, K. N.; Manners, I.; Leach, K. A.; Xu, T.; Russell, T. P.; Hawker, C. J. *Adv. Mater.* **2003**, *15*, 297. (c) MacLachlan, M. J.; Ginzburg, M.; Coombs, N.; Raju, N. P.; Greedan, J. E.; Ozin, G. A.; Manners, I. *J. Am. Chem. Soc.* **2000**, *122*, 3878.
(9) Houser, E. J.; Keller, T. M. *Macromolecules* **1998**, *31*, 4038.
(10) (a) Mîinea, L. A.; Sessions, L. B.; Ericson, K. D.; Glueck, D. S.; Grubbs, R. B. *Macromolecules* **2004**, *37*, 8967. (b) Grubbs, R. B. *J. Polym. Sci., Part A: Polym. Chem.* **2005**, *43*, 4323.
(11) Scholz, S.; Leech, P. J.; Englert, B. C.; Sommer, W.; Weck, M.; Bunz, U. H. F. *Adv. Mater.* **2005**, *17*, 1052.
(12) Corriu, R. J. P.; Gerbier, P.; Guerin, C.; Henner, B. *Angew. Chem., Int. Ed.* **1992**, *31*, 1195.
(13) Corriu, R. J. P. *Angew. Chem., Int. Ed.* **2000**, *39*, 1376.
(14) Corriu, R. J. P.; Devylder, N.; Guerin, C.; Henner, B.; Jean, A. *J. Organomet. Chem.* **1996**, *509*, 249.
(15) Yajima, S.; Omori, M. *Nature* **1977**, *267*, 823.
(16) Ungurenasu, C. *Macromolecules* **1996**, *29*, 7297.
(17) Seyferth, D.; Czubarow, P. *Chem. Mater.* **1994**, *6*, 10.
(18) Leslie-Pelecky, D. L.; Rieke, R. D. *Chem. Mater.* **1996**, *8*, 1770.
(19) (a) Lu, J. Q.; Kopley, T. E.; Moll, N.; Roitman, D.; Chamberlin, D.; Fu, Q.; Liu, J.; Russell, T. P.; Rider, D. A.; Manners, I.; Winnik, M. A. *Chem. Mater.* **2005**, *17*, 2227. (b) Lastella, S.; Mallick, G.; Woo, R.; Karna, S. P.; Rider, D. A.; Manners, I.; Jung, Y. J.; Ryu, C. Y.; Ajayan, P. M. *J. Appl. Phys.* **2006**, *99*, 024302. (c) Lu, J.; Kopley, T.; Dutton, D.; Liu, J.; Qian, C.; Son, H.; Dresselhaus, M.; Kong, J. *J. Phys. Chem. B* **2006**, *110*, 10585. (d) Hinderling, C.; Keles, Y.; Stöckli, T.; Knapp, H. F.; de los Arcos, T.; Oelhafen, P.; Korczagin, I.; Hempenius, M. A.; Vancso, G. J.; Pugin, R.; Heinzelmann, H. *Adv. Mater.* **2004**, *16*, 876.
(20) (a) Tang, B.-Z.; Petersen, R.; Foucher, D. A.; Lough, A.; Coombs, N.; Sodhi, R.; Manners, I. *J. Chem. Soc., Chem. Commun.* **1993**, 523. (b) Petersen, R.; Foucher, D. A.; Tang, B.-Z.; Lough, A.; Raju, N. P.; Greedan, J. E.; Manners, I. *Chem. Mater.* **1995**, *7*, 2045.
(21) (a) Ginzburg, M.; MacLachlan, M. J.; Yang, S. M.; Coombs, N.; Coyle, T. W.; Raju, N. P.; Greedan, J. E.; Herber, R. H.; Ozin, G. A.; Manners, I. *J. Am. Chem. Soc.* **2002**, *124*, 2625. (b) Kulbaba, K.; Resendes, R.; Cheng, A.; Bartole, A.; Safa-Sefat, A.; Coombs, N.; Stover, H. D. H.; Greedan, J. E.; Ozin, G. A.; Manners, I. *Adv. Mater.* **2001**, *13*, 732. (c) Kulbaba, K.; Cheng, A.; Bartole, A.; Greenberg, S.; Resendes, R.; Coombs, N.; Safa-Sefat, A.; Greedan, J. E.; Stöver, H. D. H.; Ozin, G. A.; Manners, I. *J. Am. Chem. Soc.* **2002**, *124*, 12522.
(22) Berenbaum, A.; Ginzburg-Margau, M.; Coombs, N.; Lough, A. J.; Safa-Sefat, A.; Greedan, J. E.; Ozin, G. A.; Manners, I. *Adv. Mater.* **2003**, *15*, 51.
(23) Liu, K.; Clendenning, S. B.; Friebe, L.; Chan, W. Y.; Zhu, X. B.; Freeman, M. R.; Yang, G. C.; Yip, C. M.; Grozea, D.; Lu, Z.-H.; Manners, I. *Chem. Mater.* **2006**, *18*, 2591.
(24) (a) Sun, Q.; Lam, J. W. Y.; Xu, K.; Xu, H.; Cha, J. A. K.; Wong, P. C. L.; Wen, G.; Zhang, X.; Jing, X.; Wang, F.; Tang, B. Z. *Chem. Mater.* **2000**, *12*, 2617. (b) Sun, Q.; Xu, K.; Peng, H.; Zheng, R.; Häussler, M.; Tang, B. Z. *Macromolecules* **2003**, *36*, 2309.
(25) Cheng, A. Y.; Clendenning, S. B.; Yang, G. C.; Lu, Z.-H.; Yip, C. M.; Manners, I. *Chem. Commun.* **2004**, 780.
(26) Clendenning, S. B.; Fournier-Bidoz, S.; Pietrangelo, A.; Yang, G. C.; Han, S. J.; Brodersen, P. M.; Yip, C. M.; Lu, Z.-H.; Ozin, G. A.; Manners, I. *J. Mater. Chem.* **2004**, *14*, 1686.
(27) Jalil, M. B. A. *IEEE Trans. Magn.* **2002**, *38*, 2613.
(28) (a) Corbierre, M. K.; Beerens, J.; Lennox, R. B. *Chem. Mater.* **2005**, *17*, 5774. (b) Johnson, B. F. G.; Sanderson, K. M.; Shephard, D. S.; Ozkaya, D.; Zhou, W. Z.; Ahmed, H.; Thomas, M. D. R.; Gladden, L.; Mantle, M. *Chem. Commun.* **2000**, 1317.
(29) Seidel, R.; Duesberg, G. S.; Unger, E.; Graham, A. P.; Liebau, M.; Kreupl, F. *J. Phys. Chem. B* **2004**, *108*, 1888.
(30) Tuan, H. Y.; Lee, D. C.; Hanrath, T.; Korgel, B. A. *Chem. Mater.* **2005**, *17*, 5705.

concerned with low-molecular-weight Ni compounds such as Ni(II) stearate,[31] Ni(II) nitrate hexahydrate,[32] Ni(II) citric acid complexes.[33] To the best of our knowledge, nickel-containing polymers have not been studied as pyrolysis precursors to Ni NPs.

Recently reported Ni-containing polymers belong to the class of coordination metallopolymers. Hasse et al. reported nickel polymers in which Ni(II) ions are coordinated by Schiff base side chains.[34] Pickup et al. and Skabara et al. synthesized cross-linked polymers based on nickel dithiolene complexes that were studied electrochemically because of their low band gap properties.[35] Ramadan et al. used poly-(2-acrylamide) benzoic acid as a chelating polymer toward Ni(II) ions.[36] To the best of our knowledge, there is only one publication on the pyrolysis of Ni-containing coordination polymers. Arafa et al. reported on polycarbosilazanes whose nitrogen atoms act as ligands toward $NiCl_2$. These polymers exhibit a nickel content of ca. 18% and thermogravimetric investigation showed that the ceramic yield is 33% after heating the polymer to 500 °C.[37] However, in this publication, only the formation of NiO was observed.

Polycarbosilanes (PCS) are an interesting class of polymers with regard to metallization. In general, organosilicon polymers such as PCSs are considered to be very practical precursors to advanced metal-containing ceramics, as they possess the advantage of forming SiC-based matrixes.[38] The properties of SiC-based ceramics, especially their high ceramic yield, thermal and chemical stability, hardness, and high strength, have led to a variety of useful applications. Furthermore, the oxide-free SiC ceramic matrix shields metal NPs from oxidation. To date, metal-containing PCS-based polymers have been used as lithographic resists,[39] liquid crystals,[40] and pyrolytic precursors to SiC-based ceramic fibers and monoliths.[38] In 1996, Corriu and co-workers thermolyzed polycarbosilanes with cobalt carbonyl groups and obtained a cobalt-containing ceramic material in high yield.[14] Recently, Casado et al. reported a rhodium-containing carbosilane dendrimer,[41] and we described lithographic patterning of cobalt-containing PCS (Co-PCS).[42]

On the basis of our previous work with Co-PCS[42] and the clusterization of acetylide-substituted PFS with nickel[43] we have targeted novel nickel-containing PCS polymers (Ni-PCS) as potential polymeric precursors to ceramics containing Ni NPs. Herein, we describe the synthesis and pyrolysis studies of a series of Ni-PCS materials.

Experimental Section

Materials. Trimethylsilyl chloride $(CH_3)_3SiCl$ (98%), *n*-butyl lithium (1.6 m in hexanes), 1-chloro-1-methylsilacyclobutane, triethylsilane, *t*butylacetylene (3,3-dimethyl-1-butyne), and phenylacetylene were purchased from Aldrich. $(CH_3)_3SiCl$ and *n*-butyl lithium (1.6 m in hexanes) were used as received. 1-Chloro-1-methylsilacyclobutane, triethylsilane, *t*butylacetylene, and phenylacetylene were purified by distillation prior to use. 1-Chloro-1-methylsilacyclobutane and triethylsilane were stored under inert atmosphere. *t*Butylacetylene and phenylacetylene were stored in an inert atmosphere at room temperature in the dark. The Pt(0) catalyst used, Karstedt's catalyst (platinum-divinyltetramethyldisiloxane complex, 2.1−2.4 wt % in xylenes), was purchased from Gelest and used as received. $[CpNi(CO)]_2$ was purchased from Aldrich and purified by sublimation. Most reactions were carried out under an atmosphere of prepurified nitrogen using either a Schlenk technique or an inert-atmosphere glove box. Solvents were dried using the Grubbs method[44] or standard methods followed by distillation. The air- and moisture-stable products $(CH_2)_3Si(Me)(C{\equiv}CR)$, $[CH_2CH_2CH_2Si(Me)(C{\equiv}CR)]_n$, and $[CH_2CH_2CH_2Si(Me)\{Ni_2(Cp)_2C_2R)]_n$ were handled under air with ACS grade solvents after workup.

Techniques. *UV Lamp.* The photoirradiation experiments were carried out with Pyrex-glass-filtered emission from a HPK 125 W high-pressure mercury lamp (Philips).

Nuclear Magnetic Resonance Spectroscopy (NMR). ^1H (300 or 400 MHz) and $^{13}C\{^1H\}$ (75.4 or 100.4 MHz) NMR spectra were recorded on a Varian Gemini 300, Mercury 300, or Mercury 400 spectrometer. ^1H and ^{13}C resonances were referenced internally to the residual protonated solvent resonances. $^{29}Si\{^1H\}$ (79.4 MHz) NMR spectra were recorded on a Mercury 400 spectrometer and referenced externally to $SiMe_4$. For NMR measurements of the Ni-clusterized polymers the respective polymers were dissolved in d_6-benzene. The respective solutions were filtered through a glass microfibre filter (Whatman) in which a magnetic stir bar was wrapped. This procedure allows for the removal of colloidal magnetic material.

Infrared Spectroscopy (IR). IR spectra were recorded using a Perkin-Elmer Spectrum One FT−IR spectrometer.

Gel Permeation Chromatography (GPC). Polymer molecular weights were determined by GPC using a Viscotek GPC MAX liquid chromatograph. The GPC instrument consisted of a column heater, Ultrastyragel columns with pore sizes of 1×10^3 to 1×10^5 Å, an inline degasser, and a differential refractometer. A flow rate of 1.0 mL/min was used with ACS grade THF as the eluent. The GPC was calibrated using narrow polydispersity polystyrene standards (American Polymer Standard).

Mass Spectrometry. Mass spectra were recorded with a VG 70-250S mass spectrometer in positive ion electron impact (EI) mode.

(31) Geng, J. F.; Jefferson, D.; Johnson, B. F. G. *J. Mater. Chem.* **2005**, *15*, 844.
(32) Wang, W.-N.; Itoh, Y.; Lenggoro, I. W.; Okuyama, K. *Mater. Sci. Eng. B* **2004**, *111*, 69.
(33) Valentini, A.; Carreno, N. L. V.; Probst, L. F. D.; Leite, E. R.; Longo, E. *Microporous Mesoporous Mater.* **2004**, *68*, 151.
(34) Werner, R.; Falk, K.; Ostrovsky, S.; Haase, W. *Macromol. Chem. Phys.* **2001**, *202*, 2813.
(35) (a) Kean, C. L.; Pickup, P. G. *Chem. Commun.* **2001**, 815. (b) Kean, C. L.; Miller, D. O.; Pickup, P. G. *J. Mater. Chem.* **2002**, *12*, 2949. (c) Pozo-Gonzalo, C.; Berridge, R.; Skabara, P. J.; Cerrada, E.; Laguna, M.; Coles, S. J.; Hursthouse, M. B. *Chem. Commun.* **2002**, 2408.
(36) (a) Ramadan, T. A.; El-Atawy, S.; Moawad, H. M. *J. Appl. Polym. Sci.* **1999**, *71*, 401. (b) Ramadan, T. A.; Moawad, H. M. *J. Appl. Polym. Sci.* **1999**, *71*, 409.
(37) Arafa, I.; El-Ghanem, H.; Al-Shalabi, R. *J. Inorg. Organomet. Polym.* **2003**, *13*, 69.
(38) (a) Interrante, L. V.; Shen, Q. In *Silicon-Containing Polymers: The Science and Technology of Their Synthesis and Applications*; Jones, R. G., Ando, W., Chojnowski, J., Eds.; Kluwer Academic Publishers: Dordrecht, The Netherlands, 2000; p 247. (b) Interrante, L. V.; Rushkin, I.; Shen, Q. *Appl. Organomet. Chem.* **1998**, *12*, 695. (c) Laine, R. M.; Babonneau, F. *Chem. Mater.* **1993**, *5*, 260.
(39) Babich, E. D. *Am. Chem. Soc. Polym. Prepr.* **1998**, *39*, 532.
(40) (a) Park, S. Y.; Zhang, T.; Interrante, L. V.; Farmer, B. L. *Polymer* **2002**, *43*, 5169. (b) Park, S. Y.; Zhang, T.; Interrante, L. V.; Farmer, B. L. *Macromolecules* **2002**, *35*, 2776.
(41) Casado, M. A.; Hack, V.; Camerano, J. A.; Ciriano, M. A.; Tejel, C.; Oro, L. A. *Inorg. Chem.* **2005**, *44*, 9122.
(42) Greenberg, S.; Clendenning, S. B.; Liu, K.; Manners, I.; Aouba, S.; Ruda, H. E. *Macromolecules* **2005**, *38*, 2023.
(43) Chan, W. Y.; Clendenning, S. B.; Berenbaum, A.; Lough, A. J.; Aouba, S.; Ruda, H. E.; Manners, I. *J. Am. Chem. Soc.* **2005**, *127*, 1765.
(44) Pangborn, A. B.; Giardello, M. A.; Grubbs, R. H.; Rosen, R. K.; Timmers, F. J. *Organometallics* **1996**, *15*, 1518.

Transmission Electron Microscopy (TEM). Pyrolyzed Ni-PCS samples were ground to a fine powder and dispersed onto a carbon film covered TEM copper grid. TEM images were obtained with a Hitachi HD-2000 scanning transmission electron microscope operating at 200 kV.

Energy-Dispersive X-ray (EDX) and Elemental Mapping. Pyrolyzed Ni-PCS samples were ground to a fine powder and dispersed onto a carbon-film-covered TEM copper grid. Maps and images were recorded using a Hitachi HD-2000 scanning transmission electron microscope operating at 200 kV with a windowless X-ray detector.

Pyrolysis and Thermogravimetric Analysis (TGA). Pyrolysis and TGA of polymers were performed using a Perkin-Elmer TGA-7 analyzer under prepurified nitrogen gas at a heating rate of 10 °C/min to 400, 600, or 900 °C. The final temperature was kept for 1 or 12 h.

Powder X-ray Diffraction Analysis (PXRD). All samples were deposited onto low-background silicon sample holders and run on a Siemens/Bruker D5000 automated diffractometer using Cu K-alpha radiation (λ = 1.54059 Å) and Kevex SS Detector for elimination of Cu K-beta radiation. A step scan mode was used for data collection with step size of 0.02° 2θ and counting time of 5−7 s per step. The primary phase identification was done via Search-Match option in Eva (version 8.0) data processing software. A Rietveld approach was employed for quantitative phase analysis as well as for evaluation of more detailed physical, structural, and microstructural features of the analyzed ceramics. The latter was carried out by Topas (version 2.1) profile fitting software[45] using a fundamental parameter approach (FPA). The initial structural models for the designated components were taken from ICSD Database (release 2/2005). The domain sizes were evaluated as mean volume weighted columns. The final values are the averaged ones in the refinement procedure. The lattice microdisorder (strain, e_0) is calculated as 50% probability of distortion of the $\Delta d/d$ values in the 3D directions.

The calculation of the mean domain size is a standard feature implemented in Topas software[45] as a common refinable parameter. The software calculates and refines all refinable parameters until the best fit (minimum differences) is achieved. All refinable parameters are listed with their calculated errors (ESD). The main domain size is calculated as volume-weighted columns of stacked lattices oriented against the primary beam in the way to provide diffraction from certain atomic planes (*hkl*). The obtained final "*L*" (nm) is the average one calculated from many different reflections (different *hkl*'s).

Differential Scanning Calorimetry (DSC). DSC analyses were performed using a TA Instruments DSC2920 modulated DSC under prepurified nitrogen gas at a scan rate of 5 °C/min from −30 to 100 °C.

Magnetization Measurements. Magnetic measurements were carried out using a Quantum Design (MPMS) superconducting quantum interference device (SQUID) magnetometer. The zero-field-cooling and field-cooling (ZFC-FC) studies of temperature-dependent magnetization were performed in a 50 Oe field between 5 and 325 K. The hysteresis studies were performed at 5 and 300 K.

Synthesis and Characterization of Acetylide-Substituted 1-Silacyclobutanes 2a and 2b. *Synthesis of **2a** and **2b**.* In the absence of light, *n*BuLi (24.9 mL, 1.6 m in hexanes, 39.8 mmol) was added within 10 min dropwise to a stirred solution of the acetylene compound HC≡CR (for **2a**, R = phenyl, 4.87 mL, 4.53 g, 44.35 mmol; for **2b**, R = ^{t}butyl, 5.40 mL, 3.64 g, 44.35 mmol) in 250 mL of Et_2O at 0 °C. The mixture was stirred for 2 h. In a separate flask, $(CH_2)_3SiMeCl$ (**1**) (5.10 mL, 6.07 g, 50.4 mmol) in 500 mL of Et_2O was cooled to ca. −78 °C, and the LiC≡CR suspension was added dropwise. The reaction mixture was allowed to warm to room temperature over ca. 4 h, at which point ca. 3 mL chlorotrimethylsilane was added to destroy any unreacted LiC≡CR. The ether solution was filtered to remove the white precipitate (LiCl). All volatile material was removed in vacuum, leaving behind slightly yellow oils. In the preparation of **2b**, the removal of residual material under a vacuum had to be carefully controlled, as **2b** is volatile itself. The products **2a** and **2b** were stored in air in the absence of light. Yields: 6.63 g, 35.6 mmol, 89% (**2a**); 5.72 g, 34.4 mmol, 86% (**2b**).

Scheme 2. Synthesis of Nickel-Clustered Polycarbosilanes (Ni-PCS) with Variable Molecular Weights and Two Substituents R = Phenyl (a) and ^{t}Butyl (b)

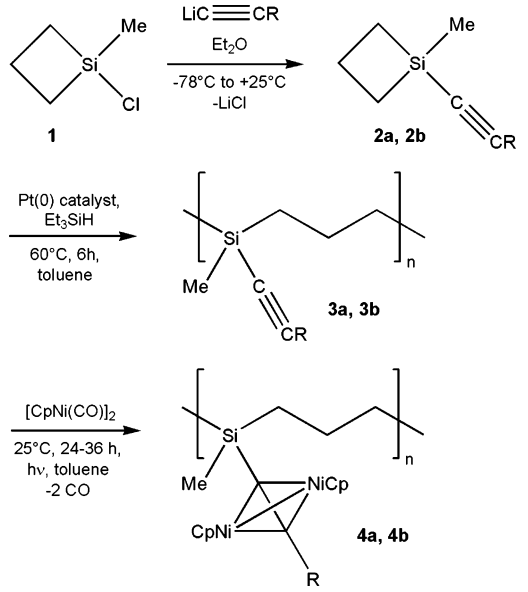

*Analytical Data for **2a**.* ^{1}H NMR (400 MHz, C_6D_6, 25 °C): δ 7.48−7.43 (m, 2H, Ph), 6.94−6.84 (m, 3H, Ph), 2.31−2.19 (m, 1H, $SiCH_2CH_2CH_2$), 2.11−2.00 (m, 1H, $SiCH_2CH_2CH_2$), 1.44−1.34 (m, 2H, $SiCH_2CH_2CH_2$), 1.11−1.02 (m, 2H, $SiCH_2CH_2CH_2$), 0.39 (s, 3H, CH_3). $^{13}C\{^1H\}$ NMR (75.4 MHz, C_6D_6, 25 °C): δ 132.6 (*o*-Ph), 129.3 (*p*-Ph), 128.9 (*m*-Ph), 123.7 (*i*-Ph), 108.3 (PhCCSi), 93.2 (PhCCSi), 19.2 ($SiCH_2CH_2CH_2$), 16.1 ($SiCH_2CH_2CH_2$), 0.3 (CH_3). $^{29}Si\{^1H\}$ NMR (79.3 MHz, C_6D_6, 25 °C): δ −6.8. FT−IR (25 °C, hexanes) ν(C≡C) = 2159 (s) cm^{-1}. MS (70 eV, EI) *m*/*z* (%) 186 (41) $[M]^+$, 158 (100) $[M - CH_2CH_2]^+$, 143 (82) $[M - CH_2CH_2 - Me]^+$. HRMS (70 eV, EI): calcd for $C_{12}H_{14}Si$, 186.086479; found, 186.086537; fit −0.3 ppm.

*Analytical Data for **2b**.* ^{1}H NMR (300 MHz, C_6D_6, 25 °C): δ 2.33−2.13 (m, 1H, $SiCH_2CH_2CH_2$), 2.10−1.91 (m, 1H, $SiCH_2CH_2CH_2$), 1.43−1.28 (m, 2H, $SiCH_2CH_2CH_2$), 1.16 (s, 9H, $C(CH_3)_3$), 1.09−0.95 (m, 2H, $SiCH_2CH_2CH_2$), 0.36 (s, 3H, $Si-CH_3$). $^{13}C\{^1H\}$ NMR (75.4 MHz, C_6D_6, 25 °C): δ 118.2 (^{t}BuCCSi), 81.1 (^{t}BuCCSi), 30.9 ($C(CH_3)_3$), 28.4 ($C(CH_3)_3$), 18.6 ($SiCH_2CH_2CH_2$), 15.9 ($SiCH_2CH_2CH_2$), 0.2 (CH_3). $^{29}Si\{^1H\}$ NMR (79.3 MHz, C_6D_6, 25 °C): δ −8.1. MS (70 eV, EI) *m*/*z* (%) 166 (4) $[M]^+$, 138 (100) $[M - CH_2CH_2]^+$, 123 (81) $[M - CH_2CH_2 - Me]^+$. HRMS: (70 eV, EI) calcd for $C_{10}H_{18}Si$, 166.117779; found, 166.118502; fit −4.3 ppm. FT−IR (25 °C, hexanes): ν(C≡C) = 2156 (s) cm^{-1}.

Synthesis and Characterization of Acetylide-substituted Polycarbosilanes (PCS) 3a and 3b with Molecular-Weight Control by the Addition of Triethylsilane Et_3SiH. *Synthesis of **3a** and **3b**.* The same procedures were used for the monomer/Et_3SiH ratios

(45) *Topas, version 2.1, General Profile and Structure Analysis Software for Powder Diffraction Data, User's Manual*; Bruker AXS GmbH: Karlsruhe, Germany, 2003.

of 10:1, 30:1, and 60:1. The following procedure for a ratio of 10:1 is typical. A mixture of silacyclobutane monomer **2a** or **2b** (5.37 mmol) and Et_3SiH (85 μL, 0.54 mmol) was stirred in 2 mL of toluene at 60 °C in the presence of Karstedt's catalyst (50 μL, ca. 0.1 wt % monomer) overnight. The colorless solution turned yellow. The resulting viscous solution was precipitated into a vortex of rapidly stirring methanol and isolated as a yellowish gummy material. The yields were 61−67% for **3a**, and 53−66% for **3b**.

Molecular-weight control was demonstrated over the range of $6340 < M_n < 33\,790$ (**3a**) and $8420 < M_n < 31\,440$ (**3b**), as measured by polystyrene-calibrated GPC. We assume that the end groups present are a mixture of Si−H and Si−OMe groups, as detected for related materials.[42]

*Analytical Data for **3a***. ^{1}H NMR (400 MHz, C_6D_6, 25 °C): δ 7.55−7.45 (m, 2H, Ph), 6.94−6.83 (m, 3H, Ph), 2.04−1.82 (m, 2H, $SiCH_2CH_2CH_2$), 1.08−0.84 (m, 4H, $SiCH_2CH_2CH_2$), 0.33 (s, 3H, CH_3). $^{13}C\{^1H\}$ NMR (75.4 MHz, C_6D_6, 25 °C): δ 132.3 (*o*-Ph), 128.5 (*m*/*p*-Ph), 123.9 (*i*-Ph), 107.2 (Ph*C*CSi), 93.3 (PhC*C*Si), 19.6 ($SiCH_2CH_2CH_2$), 19.3 ($SiCH_2CH_2CH_2$), −3.0 (CH_3). $^{29}Si\{^1H\}$ NMR (79.3 MHz, C_6D_6, 25 °C): δ −14.8. FT−IR (25 °C, hexanes): ν(C≡C) = 2159 (m) cm^{-1}. DSC (M_n = 28 760, PDI = 2.52): T_g = −3 °C. GPC: $6340 < M_n < 33\,790$; $35\,730 < M_w < 81\,140$; 2.40 < PDI < 5.63.

TGA (M_n = 6340, PDI = 5.63): T_{10} = 375 °C, T_{50} = 465 °C, maximum weight loss at 470 °C, final ceramic yield at 900 °C = 19%.

TGA (M_n = 28760, PDI = 2.52): T_{10} = 405 °C, T_{50} = 480 °C, maximum weight loss at 470 °C, final ceramic yield at 900 °C = 32%.

TGA (M_n = 33780, PDI = 2.40): T_{10} = 400 °C, T_{50} = 480 °C, maximum weight loss at 470 °C, final ceramic yield at 900 °C = 28%.

*Analytical Data for **3b***. ^{1}H NMR (300 MHz, C_6D_6, 25 °C): δ 1.93−1.80 (m, 2H, $SiCH_2CH_2CH_2$), 1.27 (s, 9H, $C(CH_3)_3$), 1.02−0.84 (m, 4H, $SiCH_2CH_2CH_2$), 0.32 (s, 3H, CH_3). $^{13}C\{^1H\}$ NMR (75.4 MHz, C_6D_6, 25 °C): δ 117.2 (^{t}BuCCSi), 81.2 (^{t}BuCCSi), 31.3 ($C(CH_3)_3$), 28.5 ($C(CH_3)_3$), 19.9 ($SiCH_2CH_2CH_2$), 19.2 ($SiCH_2CH_2CH_2$), −2.7 (CH_3). $^{29}Si\{^1H\}$ NMR (79.3 MHz, C_6D_6, 25 °C): δ −16.3. FT−IR (25 °C, hexanes) ν(C≡C) = 2154 (m) cm^{-1}. DSC (M_n = 31 440, PDI = 2.59): T_g = −21 °C. GPC: $8420 < M_n < 31\,440$; $16\,410 < M_w < 51\,180$; 1.95 < PDI < 2.59.

TGA (M_n = 8420, PDI = 1.95): T_{10} = 365 °C, T_{50} = 435 °C, maximum weight loss at 440 °C, final ceramic yield at 900 °C = 17%.

TGA (M_n = 20 920, PDI = 2.45): T_{10} = 365 °C, T_{50} = 425 °C, maximum weight loss at 440 °C, final ceramic yield at 900 °C = 12%.

TGA (M_n = 31 440, PDI = 2.59): T_{10} = 370 °C, T_{50} = 435 °C, maximum weight loss at 440 °C, final ceramic yield at 900 °C = 18%.

Synthesis and Characterization of Nickel-Clusterized PCS (Ni-PCS) 4a and 4b. *Reaction of **3** with [CpNi(CO)]$_2$: Synthesis of Ni-PCS **4a** and **4b***. The dimeric Ni complex $[CpNi(CO)]_2$ (84 mg, 0.28 mmol) and PCS **3a** (50 mg, 0.27 mmol, M_n = 6340−33790) were dissolved in 5 mL of dry toluene under a N_2 atmosphere. The reaction mixture was irradiated by a mercury lamp at 25 °C. Evolving CO was released through an oil bubbler. After light exposure for 24−36 h, the dark red solution turned into dark green. The solution containing the product was precipitated twice into a vortex of rapidly stirring methanol, and the obtained polymer was washed twice with methanol. The product was isolated by decanting, followed by drying in a high vacuum, to give a green material. Yield: 65−72 mg (55−61%) (**4a**). **4b** was prepared similarly to **4a**.

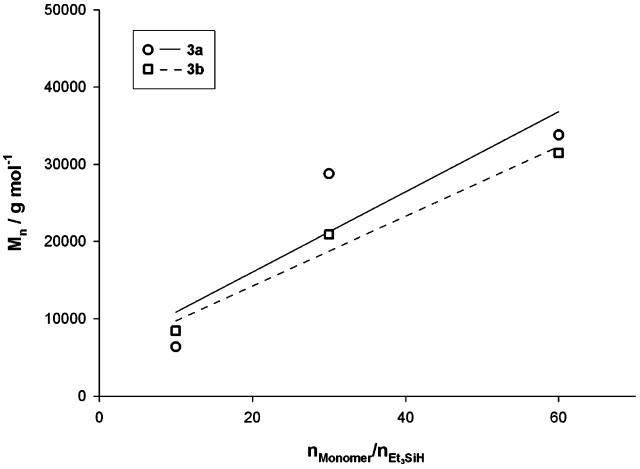

Figure 1. Molecular-weight control in Pt(0)-catalyzed polymerization of **2a** and **2b** to **3a** and **3b** by adjustment of the molar ratio $n_{monomer}/n_{Et_3SiH}$ (M_n determined by polystyrene-calibrated GPC).

*Analytical Data for **4a***. ^{1}H NMR (400 MHz, C_6D_6, 25 °C): δ 7.79 (m, Ph_{Ni}), 7.49 (m, $Ph_{no\ Ni}$), 7.20 (m, Ph_{Ni}), 6.93 (m, $Ph_{no\ Ni}$), 5.25 (s, $Ni(C_5H_5)$), 2.05−1.60 (m_{br}, $SiCH_2CH_2CH_2$), 1.20−0.80 (m_{br}, $SiCH_2CH_2CH_2$), 0.48−0.46 (m, Me_{Ni}), 0.36−0.31 (m, $Me_{no\ Ni}$). $^{13}C\{^1H\}$ NMR (100.5 MHz, C_6D_6, 25 °C) δ = 139.5 (Ph*C*(NiCp)C(NiCp)Si), 132.3 (*o*-$Ph_{no\ Ni}$), 131.3 (*o*-Ph_{Ni}), 128.5 (*m*/*p*-$Ph_{Ni\ and\ no\ Ni}$), 123.9 (*i*-$Ph_{no\ Ni}$), 123.8 (*i*-Ph_{Ni}), 113.4 (PhC(NiCp)-*C*(NiCp)Si), 107.2 (Ph*C*CSi), 93.3 (PhC*C*Si), 87.7 (C_5H_5), 22.2 ($SiCH_2CH_2CH_{2,\ Ni}$), 21.6 ($SiCH_2CH_2CH_{2,\ Ni}$), 20.3 ($SiCH_2CH_2CH_2$, Ni), 19.8 ($SiCH_2CH_2CH_{2,\ Ni}$), 19.6 ($SiCH_2CH_2CH_{2,\ no\ Ni}$), 19.3 ($SiCH_2CH_2CH_{2,\ no\ Ni}$), −1.5 ($Me_{Ni}$), −3.0 ($Me_{no\ Ni}$). $^{29}Si\{^1H\}$ NMR (79.3 MHz, C_6D_6, 25 °C): δ −14.9 (no Ni), −14.8 (no Ni), 0.4 (Ni). FT−IR (25 °C, hexanes): $\nu(C{\equiv}C_{no\ Ni})$ = 2159 (s) cm^{-1}. DSC (M_n = 11 590, PDI = 2.75): T_g = 29 °C. GPC: $8900 < M_n < 24\,070$; $23\,390 < M_w < 51\,870$; 2.16 < PDI < 2.73.

TGA (M_n = 8890, PDI = 2.63): T_{10} = 260 °C, maximum weight loss at 320 °C, ceramic yield at 400 °C = 72%; at 600 °C = 65%; at 900 °C = 61%.

TGA (M_n = 11 590, PDI = 2.75): T_{10} = 305 °C, maximum weight loss at 325 °C, ceramic yield at 400 °C = 73%; at 600 °C = 64%; at 900 °C = 57%.

*Analytical Data for **4b***. ^{1}H NMR (400 MHz, C_6D_6, 25 °C): δ 5.31 (s, $Ni(C_5H_5)$), 2.05 − 1.60 (m, $SiCH_2CH_2CH_2$), 1.37 (br s, $C(CH_3)_{3,Ni}$), 1.29 (m, $C(CH_3)_{3,no\ Ni}$), 1.21 − 0.80 (m, $SiCH_2CH_2CH_2$), 0.53 (s, Me_{Ni}), 0.48 (s, Me_{Ni}), 0.43 (s, Me_{Ni}), 0.36 (s, $Me_{no\ Ni}$), 0.32 (s, $Me_{no\ Ni}$), 0.28 (s, $Me_{no\ Ni}$). $^{13}C\{^1H\}$ NMR (100.5 MHz, C_6D_6, 25 °C): δ 134.6 (^{t}BuC(NiCp)*C*(NiCp)Si), 117.2 (^{t}BuCCSi), 90.1 (^{t}Bu*C*(NiCp)C(NiCp)Si), 87.3 (C_5H_5), 81.0 (^{t}BuCCSi), 34.6 ($C(CH_3)_{3,\ Ni}$), 33.6 ($C(CH_3)_{3,\ Ni}$), 31.3 ($C(CH_3)_{3,\ no\ Ni}$), 30.5 ($C(CH_3)_{3,\ Ni}$), 28.5 ($C(CH_3)_{3,\ no\ Ni}$), 22.7 ($SiCH_2CH_2CH_{2,\ Ni}$), 22.0 ($SiCH_2CH_2CH_{2,\ Ni}$), 20.8 ($SiCH_2CH_2CH_{2,\ Ni}$), 19.9 ($SiCH_2CH_2CH_{2,\ no\ Ni}$), 19.2 ($SiCH_2CH_2CH_{2,\ no\ Ni}$), −1.2 ($Me_{Ni}$), −2.5 ($Me_{no\ Ni}$). $^{29}Si\{^1H\}$ NMR (79.3 MHz, C_6D_6, 25 °C) δ = −16.3 (no Ni), −16.4 (no Ni), −7.1 (Ni), −7.2 (Ni). FT−IR (25 °C, hexanes): $\nu(C{\equiv}C_{no\ Ni})$ = 2154 (s) cm^{-1}. DSC (M_n = 22 130, PDI = 2.55): T_g = 25 °C. GPC: $13\,840 < M_n < 35\,850$; $21\,000 < M_w < 73\,660$; 1.52 < PDI < 2.56.

TGA (M_n = 24380, PDI = 2.21): T_{10} = 245 °C, maximum weight loss at 355 °C, ceramic yield at 400 °C = 67%; at 600 °C = 53%; at 900 °C = 51%.

Synthesis and Characterization of Ceramics from the Pyrolysis of Ni-PCSs. Pyrolysis of solvent-free Ni-PCSs was performed using a Perkin-Elmer TGA-7 analyzer under prepurified nitrogen gas at a heating rate of 10 °C/min to 400, 600, or 900 °C. The final temperature was held constant for 1 or 12 h. TEM, EDX,

Table 1. Ceramic Yield (%) and Nanoparticle Size Range (nm) of Pyrolyzed 4a and 4b at the Pyrolysis Temperatures 400, 600, and 900 °C (pyrolysis for 1 h if not marked otherwise[a])

	4a	4a	4b
M_n	8890	11 590	24 380
Ni clusterization (%)	23	28	37
ceramic yield[b] at 400 °C (%)	72	72	67
ceramic yield[b] at 600 °C (%)	64	65	53, 46[a]
ceramic yield[b] at 900 °C (%)	60	61	49
NP size range[c] at 400 °C (nm)	2−4	2−3	2−5
NP size range[c] at 600 °C (nm)	2−5, 15−30	3−4, 10−35	2−6, 2−10,[a] 25−100[a]
NP size range[c] at 900 °C (nm)	100−200	3−4, 20−60	3−8, 30−60

[a] Pyrolysis for 12 h. [b] Determined by thermogravimetric analysis (TGA). [c] Determined by transmission electron microscopy (TEM).

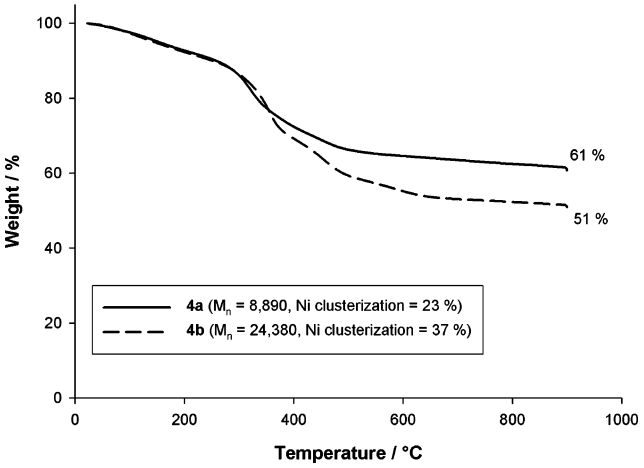

Figure 2. Thermogravimetric analysis (TGA) of Ni-PCSs **4a** and **4b**.

elemental mapping, PXRD, and SQUID were used to characterize the ceramic materials obtained from pyrolysis of Ni-PCSs **4a** and **4b**.

Results and Discussion

Synthesis and Characterization of Ni-PCSs 4a and 4b. The synthesis of nickel-containing polycarbosilanes (Ni-PCS) **4a** and **4b** started from commercially available 1-chloro-1-methylsilacyclobutane **1** (Scheme 2). Reaction of **1** with two different lithium acetylides (R = Ph (a) and ^{t}Bu (b)) in diethyl ether gave the two acetylide substituted silacyclobutane monomers **2a** and **2b** in yields of 89 and 87%. Both monomers were characterized by ^{1}H NMR, ^{13}C NMR, and ^{29}Si NMR spectroscopy, FT−IR, and mass spectrometry.

In the syntheses of **2a** and **2b**, a slight excess of **1** with respect to the lithium acetylides was used to avoid anionic initiation[46] of ring-opening polymerization of **1** and **2**. Polymerization of the silacyclobutanes **2a** and **2b** was carried out by Pt(0) catalysis (Karstedt's catalyst, 0.1 wt % with respect to monomer) under molecular-weight control conditions. The applied method is known from molecular-weight control of, e.g., oligocarbosilanes,[42,47] polyferrocenylsilanes,[48,49] and Co-PCS.[42] We assume that a mechanism operates that is similar to that in the case of [1]ferrocenophane polymerization.[48] By the addition of various amounts of triethylsilane Et_3SiH ($n_{monomer}/n_{Et_3SiH}$ = 10, 30, and 60) to the polymerization mixture (monomer **2a** or **2b**, Pt(0) catalyst, and toluene) the molecular weights of the obtained polycarbosilanes **3a** and **3b** were adjusted in the range of $6340 < M_n < 33\,790$ (**3a**) and $8420 < M_n < 31\,440$ (**3b**) as determined by polystyrene calibrated GPC (Figure 1). The molecular-weight distributions of the PCSs were rather broad, as evidenced by the polydispersity indices (PDI): 2.4−5.6 (**3a**), 2.0−2.6 (**3b**). The acetylide-substituted PCSs **3a** and **3b** were characterized by ^{1}H NMR, ^{13}C NMR, and ^{29}Si NMR spectroscopy, FT−IR, DSC, and GPC.

In the last synthetic step of the Ni-PCS synthesis, PCSs **3a** and **3b** were clustered by reaction with the dimeric nickel complex $[CpNi(CO)]_2$, yielding Ni-PCSs **4a** and **4b** as green solids. In principle, this clusterization reaction can be carried out thermally or photolytically.[50] In a first comparative test reaction of Ni clusterization of **3a** by means of photolysis at 25 °C and thermal clusterization at 60 °C, photoclusterization turned out to be faster and yielded higher amounts of Ni incorporation. Photoclusterization in toluene at room temperature for 13 h gave a percentage of Ni clusterization of 29%. Thermal clusterization for 2 days at 60 °C yielded only 16% metallization of the acetylide groups. Accordingly, the photochemical route was chosen for all Ni−PCS syntheses.

The degree of Ni clusterization of **4a** and **4b** was determined by ^{1}H NMR spectroscopy. Quantitative comparison of the integrals of the cyclopentadienyl (NiCp) signal (**4a**, 5.25 ppm; **4b**, 5.31 ppm) and the $CH_2-CH_2-CH_2$ methylene signal (**4a**, **4b**: 2.05−1.60 ppm) of the polymer backbone gave the clusterization percentage. To obtain useful ^{1}H NMR spectra, the benzene solutions of the Ni-PCSs had to undergo a filtration procedure to remove colloidal nickel particles, the presence of which led to considerable signal broadening. The obtained clusterization percentages for the two polymers were in the ranges of 23−33% (**4a**) and 35 − 37% (**4b**). The limitation in clusterization might be due to steric hindrance along the polymer backbone, which is more strongly pronounced with the phenyl-substituted PCSs. However, Ni clusterizations below 100% are probably beneficial with regard to the pyrolysis of the Ni-PCSs **4a** and **4b**, as remaining non-clustered C−C triple bonds are known to contribute to a high ceramic yield due to cross-linking reactions.[14] These cross-linking reactions in the matrix should also help prevent Ni NP agglomeration during the

(46) Uenishi, K.; Imae, I.; Shirakawa, E.; Kawakami, Y. *Chem. Lett.* **2001**, *30*, 986.
(47) Bamford, W. R.; Lovie, J. C.; Watt, J. A. C. *J. Chem. Soc. C* **1966**, 1137.
(48) (a) Gómez-Elipe, P.; Resendes, R.; Macdonald, P. M.; Manners, I. *J. Am. Chem. Soc.* **1998**, *120*, 8348. (b) Temple, K.; Jäkle, F.; Sheridan, J. B.; Manners, I. *J. Am. Chem. Soc.* **2001**, *123*, 1355. (c) Gómez-Elipe, P.; MacDonald, P. M.; Manners, I. *Angew. Chem., Int. Ed.* **1997**, *36*, 762.
(49) Bartole-Scott, A.; Resendes, R.; Manners, I. *Macromol. Chem. Phys.* **2003**, *204*, 1259.
(50) Forbes, E. J.; Iranpoor, N. *J. Organomet. Chem.* **1982**, *236*, 403.

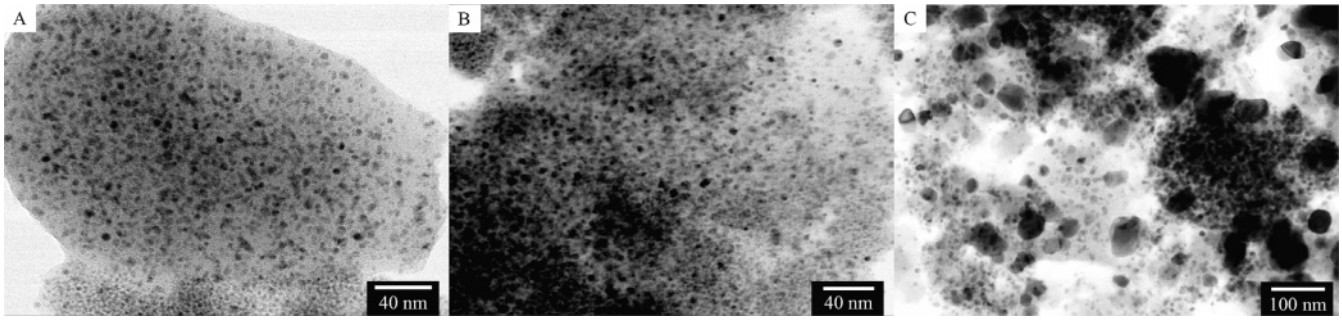

Figure 3. TEM images of pyrolyzed **4b** (M_n = 24 380, Ni clusterization = 37%), pyrolysis at (A) 400, (B) 600, and (C) 900 °C for 1 h.

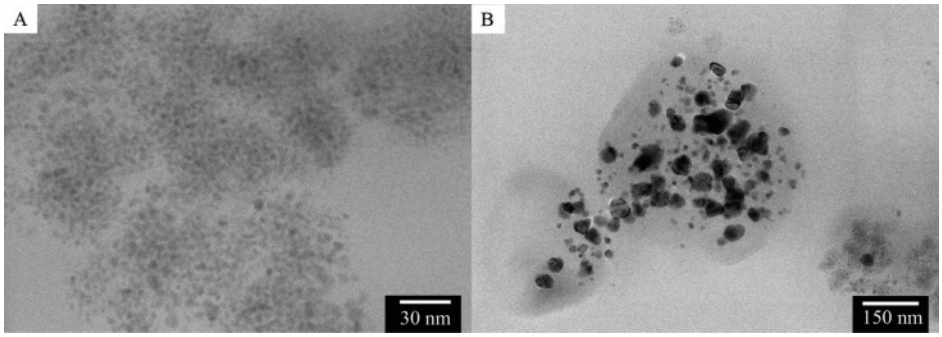

Figure 4. TEM images of pyrolyzed **4b** (M_n = 24 380, Ni clusterization = 37%), pyrolysis at 600 °C for 12 h.

pyrolysis process. Ni-PCSs **4a** and **4b** were characterized by ^{1}H NMR, ^{13}C NMR, ^{29}Si NMR spectroscopy, FT−IR, DSC, and GPC. The NMR spectra exhibited signals that could be assigned to clusterized and non-clusterized repeat units. Tacticity effects and unlike neighboring repeat units led to an increase in the number of NMR signals. Thus, it was possible to synthesize Ni-PCSs **4a** and **4b** with different alkyne substituents, and various molecular weight (**4a**, 8890 < M_n < 24 070; **4b**, 13 840 < M_n < 35 850) for further studies. The molecular weights were determined by GPC versus polystyrene standards, so the values are considered estimates.

Pyrolysis of Ni-PCSs 4a and 4b. Pyrolysis of **4a** (M_n = 8890, Ni clusterization = 23% and M_n = 11 590, Ni clusterization = 28%) and **4b** (M_n = 24 380, Ni clusterization = 37%) at 400−900 °C afforded black ceramic products. Pyrolysis was carried out for 1 h at temperatures of 400, 600, and 900 °C. To test the influence of pyrolysis time **4b** (M_n = 24 380, Ni clusterization = 37%) was also pyrolyzed for 12 h at 600 °C. A comparative overview of the obtained materials, the respective ceramic yields, and the NP size ranges is given in Table 1.

Comparison of the ceramic yields of the pyrolyzed Ni-PCS (Table 1) at the respective temperatures showed that phenyl-substituted Ni-PCSs **4a** give higher ceramic yields than ^{t}Bu-substituted Ni-PCSs **4b**. In addition, it could be shown for the pyrolysis of **4b** at 600 °C for 1 and 12 h that longer pyrolysis times result in a lower ceramic yield (Table 1).

The pyrolysis of **4a** with higher molecular weight (M_n = 11 590) and a higher percentage of nickel clusterization (28%) gave a TGA curve very similar to that obtained for the other investigated **4a** (M_n = 8890, Ni clusterization = 23%, Figure 2), within experimental error. Thus, differences in molecular weight of ca. 3000 g mol^{-1} and variations in Ni clusterization of ca. 5% do not affect the ceramic yield significantly for **4a**. Weight loss starts quite constantly from room temperature to ca. 300 °C. The maximum weight loss of **4a** (M_n = 8890, Ni clusterization = 23%) is observed at 321 °C, that of **4b** (M_n = 24 380, Ni clusterization = 37%) is at 355 °C. It is interesting to note that the maximum weight loss of **4a** is at a 35 °C lower temperature, but in the end, **4a** gives a higher ceramic yield (Figure 2).

From Figure 2, it is evident that the different ceramic yields of **4a** and **4b** are due to the substituents ^{t}Bu and Ph as **4b** (M_n = 24 380, Ni clusterization = 37%) with higher molecular weight and higher degree of clusterization than **4a** (M_n = 8890, Ni clusterization = 23%) gives a lower ceramic yield. One would expect a higher molecular weight and a higher clusterization percentage to result in a higher ceramic yield. Compared to Ni-PCSs **4**, pyrolysis of the non-clusterized PCS polymers **3** led to considerably lower ceramic yields at 900 °C of 19−32% (**3a**) and 12−18% (**3b**) with the ^{t}Bu-substituted polymer **3b** giving lower ceramic yields than the Ph-substituted PCS **3a**. For the PCS polymers **3**, the ceramic yield increases with increasing molecular weight: 19% at M_n = 6340 (**3a**) to 28% at M_n = 33 780 (**3a**) and 17% at M_n = 8420 (**3b**) to 18% at M_n = 31 440 (**3b**). All these pyrolysis results for the polymers **3** and **4** suggest that the phenyl-substituted polymers (with sp^2 carbons) give higher ceramic yields as opposed to the ^{t}Bu-substituted polymers (with sp^3 carbons), which is most likely due to the more pronounced formation of graphite during pyrolysis of the phenyl-substituted polymers.

Characterization of Ceramics Derived from Pyrolysis of Ni-PCSs 4a and 4b. *(a) Transmission Electron Microscopy (TEM).* TEM pictures of the following pyrolyzed polymer samples **4b** are discussed in order to highlight the influence of pyrolysis time and pyrolysis temperature: **4b** (M_n = 24 380, 37% Ni clusterization), 1 h pyrolysis at 400,

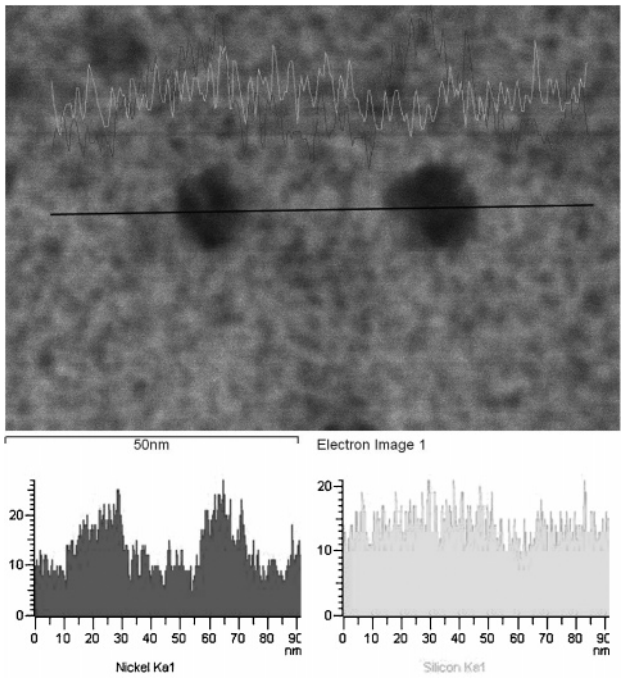

Figure 5. TEM (top) and EDX (below, for Ni and Si) of **4a** (M_n = 11 590, 28% Ni clusterization), pyrolyzed at 600 °C for 1h. The black line in the TEM picture marks the scan through the two nanoparticles.

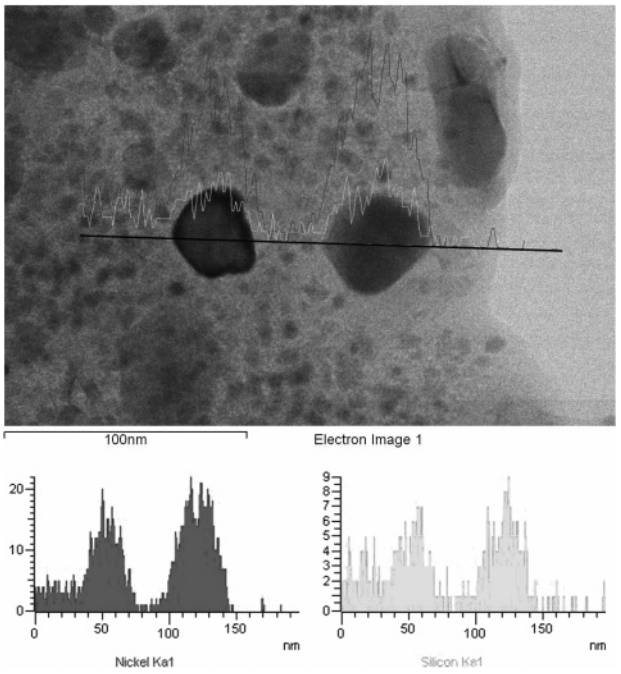

Figure 6. TEM (top) and EDX (below, for Ni and Si) of **4a** (M_n = 11 590, 28% Ni clusterization), pyrolyzed at 900 °C for 1h. The black line in the TEM picture marks the scan through the two nanoparticles.

600, and 900 °C (see Figure 3) and **4b** (M_n = 24 380, 37% Ni clusterization), 12 h pyrolysis at 600 °C (Figure 4).

In **4b** pyrolyzed at 400 °C for 1 h, NPs were discernible and very small (2−5 nm) (Figure 3). At the pyrolysis temperature of 600 °C, the formation of NPs was easily detected and the particle size was quite well-defined at ca. 2−6 nm. At the pyrolysis temperature of 900 °C, large particles up to 60 nm were also formed. Agglomeration of small particles due to further weight loss between 600 and 900 °C is most likely to be the important factor that enhances the formation of the larger NPs; this probably occurs at domain boundaries.[21a]

The influence of the pyrolysis time was studied using the sample **4b** (M_n = 24 380, Ni clusterization = 37%) as well. Two pyrolysis experiments were carried out at the temperature of 600 °C, one experiment for 1 h and the other one for 12 h. The longer pyrolysis time of 12 h gave ceramics that also contain larger NPs (25−100 nm) (Figure 4) in addition to the smaller ones (2−10 nm). Thus, a longer pyrolysis time leads to particle agglomeration because no large particles could be found after a pyrolysis time of 1 h (Figure 3b). It is most likely that during longer pyrolysis at 600 °C, the larger NPs (25−100 nm) are formed on the surface of Ni-PCS and the smaller NPs (2−10 nm) are formed in the bulk of the material. This connection between NP size and their location, either in the bulk or on the surface of materials, was shown in detail recently in studies of the pyrolysis of Co-PFS thin films.[23]

(b) Compositional Analysis of Nanoparticles. The pyrolyzed Ni-PCS samples were analyzed by energy-dispersive X-ray elemental mapping analysis (EDX). Powder X-ray diffraction (PXRD) was applied to determine the composition of the NPs.

EDX mapping analysis revealed an interesting feature of pyrolyzed **4a** (M_n = 11 590, Ni clusterization = 28%) with respect to pyrolysis temperature. At 600 °C, the EDX showed that in the particles formed, nickel is accumulated (Figure 5). In contrast, the signal for silicon does not indicate a dependence on location. However, EDX analysis of the same sample of **4a** pyrolyzed at 900 °C showed that at this temperature, the nanoparticles were rich in both nickel and silicon (Figure 6). This points to the fact that at 600 °C, nickel nanoparticles are formed, whereas at 900 °C, NPs consisting of nickel and silicon are obtained.

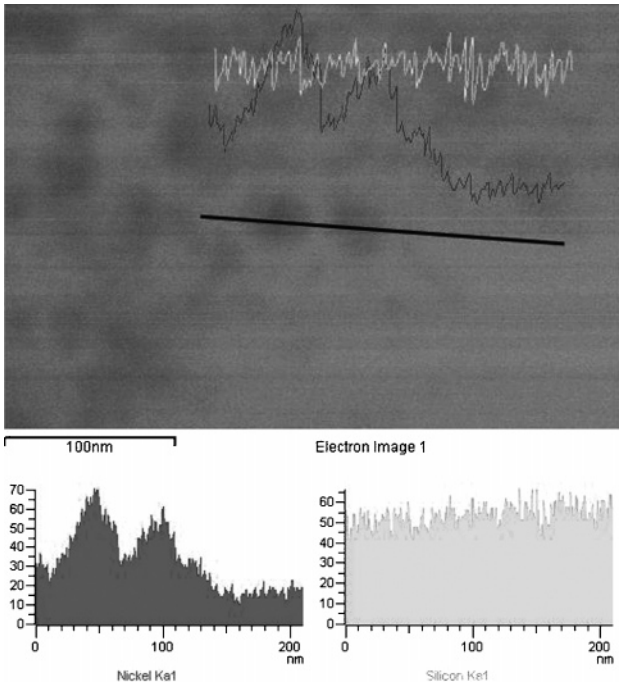

Figure 7. TEM (top) and EDX (below, for Ni and Si) of **4b** (M_n = 24 380, Ni clusterization 37%), pyrolyzed at 600 °C for 12 h. The black line in the TEM picture marks the scan through the two nanoparticles.

Table 2. PXRD Data of Pyrolyzed 4b (M_n = 24 380, Ni Clusterization = 37%) under Different Conditions

pyrolysis conditions	composition	quantity (wt %)	space group	lattice (Å)	mean domain size[a] L (nm)
600 °C/1 h	Ni	100	*Fm*3*m*	a = 3.52 (3)	5.1 (±2.2)
600 °C/12 h	Ni	99	*Fm*3*m*	a = 3.524 (3)	13.2 (±2.8)
	NiO	1	*Fm*3*m*	a = 4.178 (3)	15.5 (±3.1)
900 °C/1 h	Ni_3Si	57	*Pm*3*m*	a = 3.5137 (2)	17.2 (±3.2)
	Ni	33	*Fm*3*m*	a = 3.5144 (11)	47.5 (±5.1)
	$Ni_{31}Si_{12}$	10	*P*32	a = 6.675 (7), c = 12.254 (8)	10.2 (±3.1)

[a] For the method of determination of the mean domain size, please see the Experimental Section (PXRD).

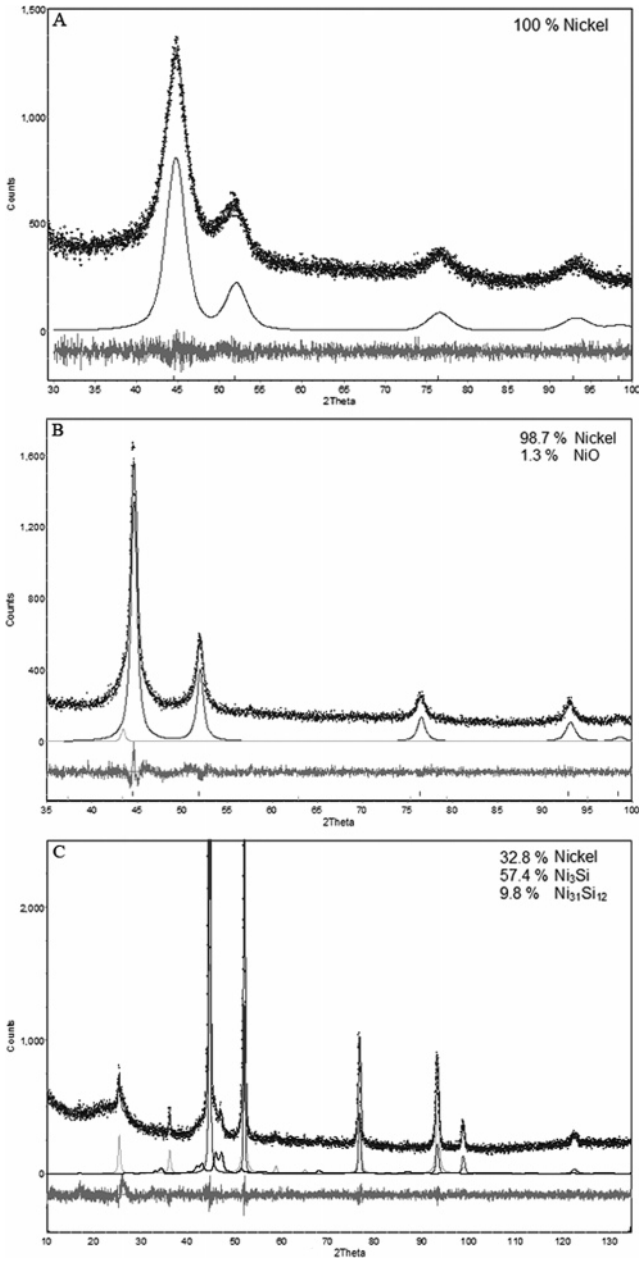

Figure 8. PXRD Rietveld plots: (A) pyrolyzed **4b** (M_n = 24 380, Ni clusterization = 37%), pyrolyzed at 600 °C for 1 h; (B) at 600 °C for 12 h; (C) at 900 °C for 1 h.

EDX of the ceramic derived from **4b** (M_n = 24 380, Ni clusterization 37%) at 600 °C for 12 h (Figure 7) showed that Ni−Si accumulation in the NPs does not depend on long pyrolysis times but on the higher temperature of 900 °C. Thus, after 12 h of pyrolysis at 600 °C, only the Ni EDX signal showed a dependence on the location.

In the Supporting Information, the nickel elemental maps of two selected samples at 600 °C are depicted (see the Supporting Information, Figures S1 and S2). The elemental mappings (EDX) in bright-field and dark-field TEM indicate that nickel atoms are accumulated in the NPs.

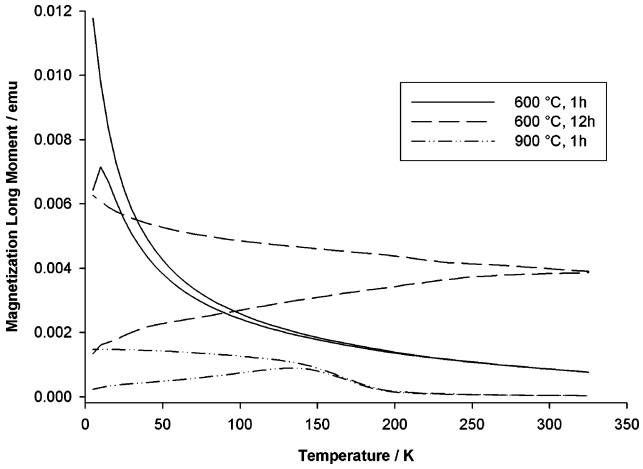

Figure 9. ZFC-FC curves (50 Oe field) of pyrolyzed **4b** (M_n = 24 380, Ni clusterization = 37%) for three different pyrolysis conditions: 600 °C/1 h, 600 °C/12 h, 900 °C/1 h.

To determine the composition of the NPs, we carried out powder X-ray diffraction (PXRD) analysis on pyrolyzed **4b** (M_n = 24 380, Ni clusterization = 37%). The influence of the pyrolysis conditions (temperature and time) was evaluated by comparing the phase composition of the NPs formed under several pyrolysis conditions: (i) pyrolysis at 600 °C for 1 h, (ii) pyrolysis at 600 °C for 12 h, (iii) pyrolysis at 900 °C for 1 h. The acquired PXRD data is summarized in Table 2.

From the data summarized in Table 2 and shown in Figure 8a−c, it can be seen that the three different pyrolysis conditions led to different compositions of the analyzed NP phases. Pyrolysis at 600 °C for 1 h produced, with experimental error, pure 100% nickel (Figure 8a). Extension of the time of pyrolysis to 12 h led to a sharp increase in the mean domain sizes of the Ni crystallites from 5.1 to 13.2 nm. In addition, formation of a small fraction (1.3%) of NiO ("Bunsenite") was detected (Figure 8b), which is most likely due to traces of oxygen in the N_2 atmosphere used for the pyrolysis experiments. Another possibility for the formation of NiO is oxidation after the ceramic is exposed to air after pyrolysis. A completely different NP phase composition was found at the pyrolysis temperature of 900 °C. The Ni crystallites grew further and reached a mean domain size of 42−53 nm and two new binary nickel-silicide phases, Ni_3Si and $Ni_{31}Si_{12}$, were formed in addition to elemental nickel (Figure 8c). The cubic Ni_3Si phase dominated over the

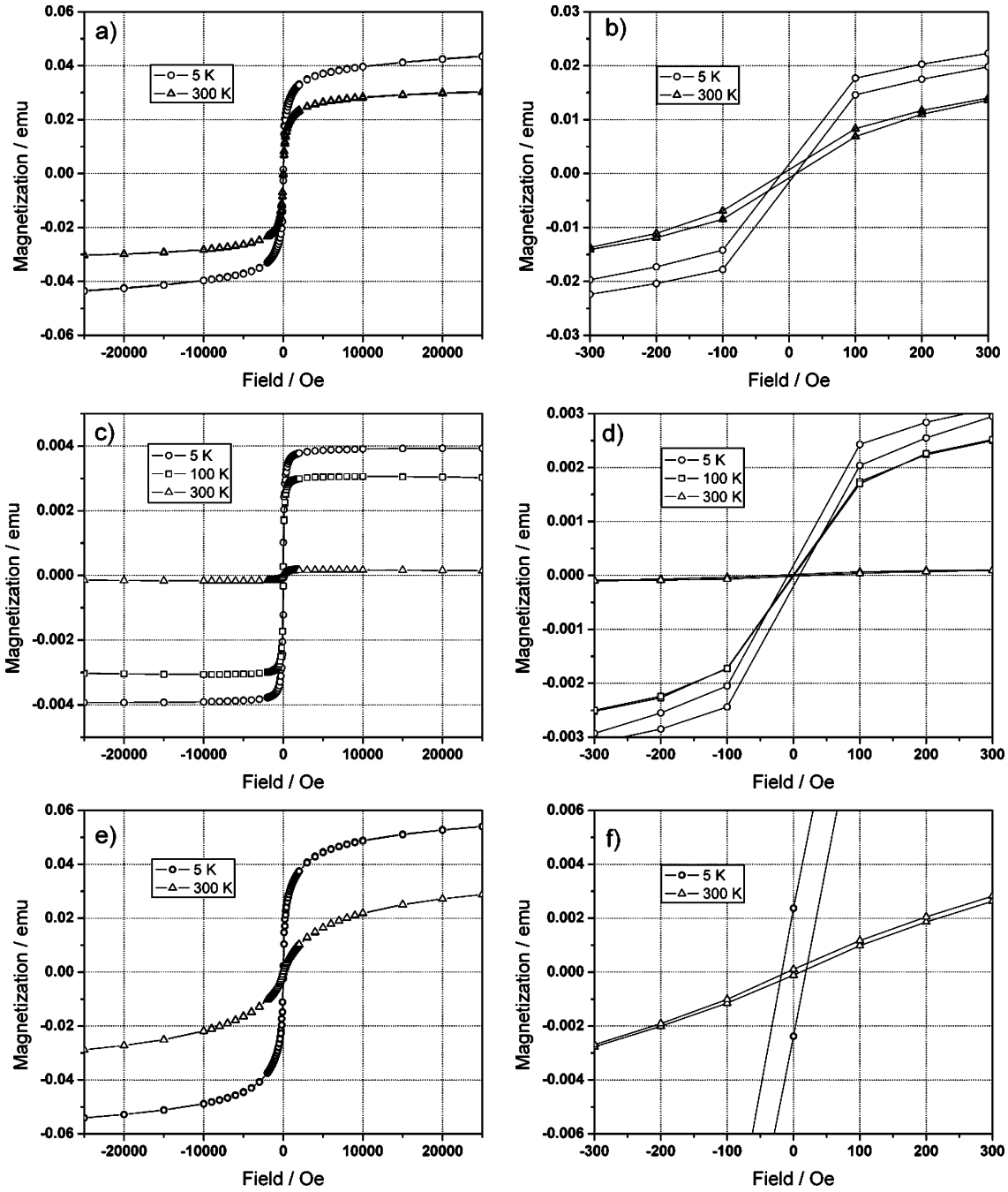

Figure 10. Magnetization vs field measurements at various temperatures of pyrolyzed **4b** (M_n = 24 380, Ni clusterization = 37%): (a) pyrolysis at 600 °C for 12 h, (c) pyrolysis at 900 °C for 1 h, (e) pyrolysis at 600 °C for 1 h, and (b, d ,f) enlargement of each origin, respectively.

rhombohedral $Ni_{31}Si_{12}$. It is known that Ni_3Si and $Ni_{31}Si_{12}$ are in equilibrium at high temperatures.[51−53] It is also worth noting that the two cubic lattices of Ni_3Si and Ni exhibit very close lattice parameters (a = 3.514 Å), which suggests a possible intergrowth between the grains with stacking alteration of both lattices along certain directions. It is a remarkable feature of the Ni_3Si phase that the Ni−Ni distances in Ni_3Si are shorter (2.4819 Å) than in the metallic Ni phase (2.492 Å).[54]

(c) Magnetic Properties of the Ceramics. The ceramic material obtained through pyrolysis (for 12 h at 600 °C) of **4b** (M_n = 24 380, Ni clusterization 37%) was readily attracted to a bar magnet. On the basis of this observation, we investigated the magnetic properties of the NP-containing ceramics by SQUID magnetometry. The focus was on the Ni and Ni-silicide containing ceramics derived from pyrolysis of **4b** (M_n = 24 380, Ni clusterization 37%). ZFC-FC (zero-field-cooled/field-cooled) measurements were carried out in order to estimate the blocking temperature T_B, as the ZFC

(51) Datta, M. K.; Pabi, S. K.; Murty, B. S. *J. Appl. Phys.* **2000**, *87*, 8393.
(52) Lauwers, A.; de Potter, M.; Chamirian, O.; Vrancken, C.; Maex, K. *Microelectron. Eng.* **2002**, *64*, 131.
(53) Frank, K.; Schubert, K. *Acta Crystallogr., Sect. B* **1971**, *27*, 916.
(54) Swanson, H. E.; Tatge, E. *Acta Crystallogr.* **1954**, *7*, 464.

(55) Jiang, J. Z.; Morup, S. *Nanostruct. Mater.* **1997**, *9*, 375; there is an uncertainty in T_B, especially in materials with broad particle size distributions. T_B also decreases with increasing magnetic field.[18]

curve peaks at T_B.[55] The estimated blocking temperatures for the respective pyrolysis conditions were $T_B \approx 10$ K (pyrolysis 600 °C for 1 h), $T_B \geq 325$ K (600 °C, 12 h), and $T_B \approx 135$ K (900 °C, 1 h) (Figure 9).

Magnetization versus field measurements were carried out at various temperatures for the three samples in order to determine the magnetic behavior above and below T_B (Figure 10a-f). For all samples, hysteresis was observed for measurements below the estimated T_B, indicating ferromagnetic behavior in that temperature range. For the two samples pyrolyzed for 1 h, hysteresis is no longer observed above T_B and the NP-containing ceramics exhibit superparamagnetic behavior.[56] These results are consistent with the sizes of the NPs observed by TEM, which are below that of a single Weiss domain of Ni (55 nm).[18]

Summary

The successful synthesis of soluble and easily processed Ni-PCSs as new precursors for the generation of ceramics containing Ni and Ni-silicide NPs has been demonstrated. These air- and moisture-stable metallopolymers were obtained via macromolecular clusterization of carbon−carbon triple bonds in acetylide-substituted PCSs. The pyrolysis of the novel Ni-PCS polymers offers the fascinating opportunity to incorporate nickel-containing nanoparticles into a ceramic matrix. Recently, we, our collaborators, and others have shown that Fe NPs derived from related ferrocenylsilane polymers are excellent catalysts for carbon nanotube growth.[2f,19] For example, small and uniform diameter single-walled carbon nanotubes can be grown in desired locations by prepatterning the polymer precursor. This has permitted the creation of 160 carbon nanotube field-effect transistors on a single silicon chip.[19b] In addition, spatially selective formation of suspended carbon nanotubes over a large surface area has been demonstrated using this approach.[19c] Ni NPs are often the catalyst of choice for CNT growth, and the new polymers reported here may prove to be even more efficient than the Fe polymers utilized previously.[29] In addition, the ability to readily pattern magnetic Ni NPs offers an opportunity to create spintronic devices, such as nanogranular in-gap structures.[27] Ni NPs differ in their magnetic properties from those of Fe NPs and may prove advantageous for this type of application. Investigations on the use of these materials as catalysts and in devices are ongoing, and our results will be addressed in future publications.

Acknowledgment. I.M. is grateful to the NSERC AGENO program for supporting this research and thanks the Canadian Government for a Canada Research Chair. I.M. also thanks the European Union for a Marie Curie Chair and the Royal Society for a Wolfson Research Merit Award. L.F. and B.O. acknowledge fellowships from the Deutscher Akademischer Austauschdienst DAAD (German Academic Exchange Service). The authors thank Kyong-Taek Kim for DSC measurements and Wing Yan Chan for helpful discussions.

Supporting Information Available: EDX element map of pyrolyzed **4a** (pyrolyzed at 600 °C for 1 h) and pyrolyzed **4b** (pyrolyze d at 600 °C for 12 h). This material is available free of charge via the Internet at http://pubs.acs.org.

CM062470J

(56) Because of equipment limitation, it was not experimentally possible to measure the magnetization curve for the 12 h sample, as T_B was above room temperature (300 K).